Обзор ArXiv:astro-ph, 11-15 марта 2019 года

От Сильченко О.К.

ArXiv: 1903.03124

WISDOM project – IV. A molecular gas dynamical measurement of the supermassive black hole mass in NGC 524

Mark D. Smith,[1⋆] Martin Bureau,[1,2] Timothy A. Davis,[3] Michele Cappellari,[1] Lijie Liu,[1] Eve V. North,[3] Kyoko Onishi,[4] Satoru Iguchi[5,6] and Marc Sarzi[7]

[1] *Sub-department of Astrophysics, Department of Physics, University of Oxford, Denys Wilkinson Building, Keble Road, Oxford, OX1 3RH, UK*

[2] *Yonsei Frontier Lab and Department of Astronomy, Yonsei University, 50 Yonsei-ro, Seodaemun-gu, Seoul 03722, Republic of Korea*

[3] *School of Physics & Astronomy, Cardiff University, Queens Buildings, The Parade, Cardiff, CF24 3AA, UK*

[4] *Research Center for Space and Cosmic Evolution, Ehime University, Matsuyama, Ehime, 790-8577, Japan*

[5] *Department of Astronomical Science, SOKENDAI (The Graduate University of Advanced Studies), Mitaka, Tokyo 181-8588, Japan*

[6] *National Astronomical Observatory of Japan, Mitaka, Tokyo, 181-8588, Japan*

[7] *Armagh Observatory and Planetarium, College Hill, Armagh, BT61 9DG, UK*

Accepted 2019 February 26. Received 2019 February 12; in original form 2018 December 13

Черная дыра в NGC 524

- По звездной кинематике (наблюдения в оптическом диапазоне) масса центральной черной дыры 800 млн солнечных масс.
- Тогда радиус ее заметной гравитации 73 пк (0.65”)
- Наблюдения линии CO на ALMA проведены с пространственным разрешением 0.3”

Наблюдения в линии CO, с ALMA

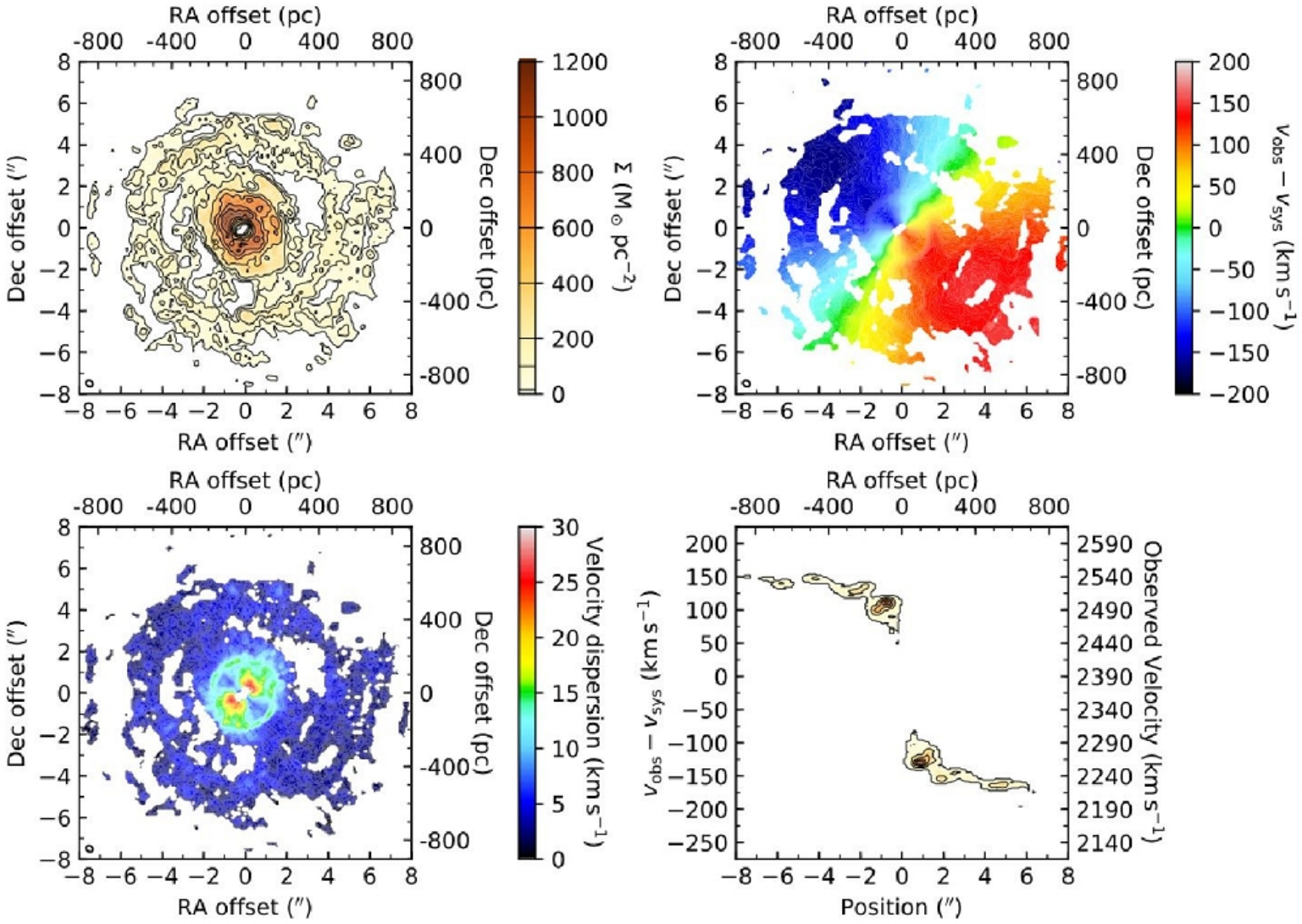

Figure 1. Moment maps of the ^{12}CO(2-1) emission in NGC 524, from our ALMA data. **Top-left:** Molecular gas surface density, assuming a CO-to-H_2 conversion factor α_{CO} =

Подгонка модели кругового вращения по трем параметрам

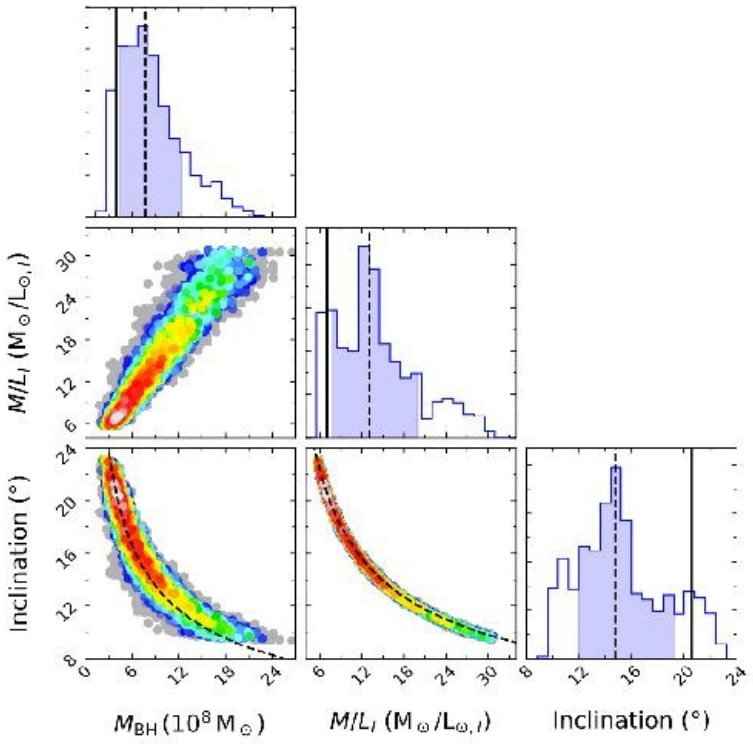

Figure 3. Corner plots showing the covariances between the three key model parameters, from a fit using the circularised MGE model permitting low inclinations. The inclination uncertainty is directly correlated with the uncertainties in both SMBH mass and stellar M/L_I. Each point is a realisation of our model, colour-coded to show the relative log-likelihood of that realisation, with white points the most likely and blue least. Grey points are realisations with $\Delta\chi^2 > \sqrt{2N}$ relative to the best-fitting model, and are even less likely. Black dashed lines on the scatter plots indicate

А это качество подгонки PV-диаграммы

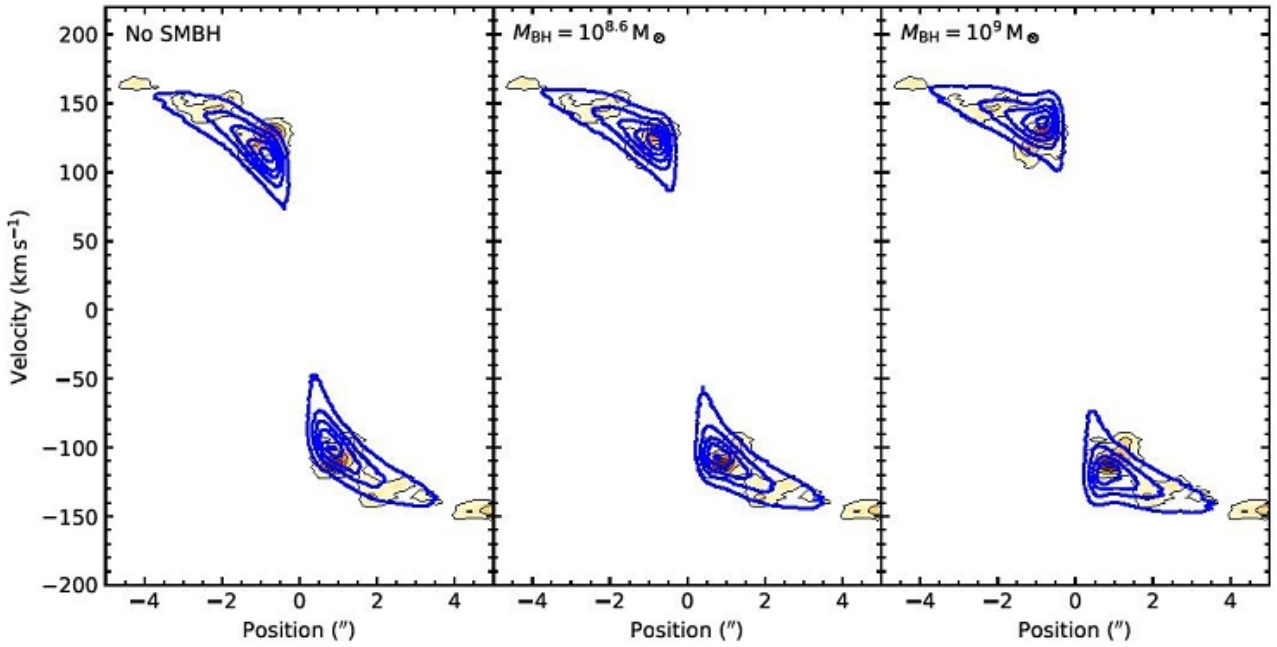

Figure 5. Model position-velocity diagrams along the kinematic major axis of the galaxy (blue contours), showing a model without a SMBH (left), with the best-fitting SMBH (centre) and with an overly large SMBH (right). These are overlaid on the observed PVD previously shown in Figure 1 (orange scales and contours). As can be seen at small radii, the line-of-sight velocities are enhanced compared to a stellar mass-only model, requiring additional central mass to fully account for them.

Все параметры модели КРУГОВОГО ВРАЩЕНИЯ ГАЗА

Table 4. Best-fitting model parameters, with associated formal uncertainties determined using the modified Bayesian sampling approach described in Section 4.3.2.

	Circularised MGE (χ^2_{red} = 1.84)				Fixed inclination (χ^2_{red} = 1.84)		
Parameter	Priors	Best fit	Median	3σ Error	Priors	Median	3σ Error
(1)	(2)	(3)	(4)	(5)	(6)	(7)	(8)
Mass model							
log(SMBH mass) ($M_\odot$)	5 → 16	8.60	8.89	±0.42	5 → 12	8.60	−0.21, +0.15
Stellar M/L_I ($M_\odot/L_{\odot,I}$)	1 → 10^7 ⋆	7.0	13.2	−7.4, +15.0	0.1 → 10	5.7	±0.3
Molecular gas geometry							
Scale length (″)	0.1 → 10	1.02	1.02	±0.1	0.1 → 10	1.1	±0.1
Truncation radius (″)	0 → 10	0.53	0.52	±0.07	0 → 10	0.51	±0.07
6.″4 × 6.″4 integrated intensity (Jy km s^{-1})	1 → 200	20.8	20.8	±1.5	1 → 200	24.7	−2.0, +1.9
Gas velocity dispersion (km s^{-1})	1 → 100	9.3	(fixed)	(fixed)	(fixed)	9.3	(fixed)
Viewing geometry							
Inclination (°)	0.1 → 90	20.6	14.8	−5, +8	(fixed)	20	(fixed)
Position angle (°)	0 → 359	39.9	39.6	±1	0 → 359	39.6	±1
Nuisance Parameters							
Centre RA offset (″)	−1 → 1	-0.12	-0.12	±0.04	(fixed)	−0.12	(fixed)
Centre Dec. offset (″)	−1 → 1	-0.05	-0.05	±0.04	(fixed)	−0.05	(fixed)
Centre velocity offset (km s^{-1})	−75 → 75	7.9	7.8	±1.5	−75 → 75	7.6	±1.2

Notes: The reduced chi–squared value given is that of the model with the best-fitting parameters for each MCMC chain. For the circularised MGE fit, the asymmetric posteriors shown in Figure 3 mean that the minimum chi-squared and the median of the 1D marginalisation of each parameter are not the same, so both are listed. In both fits, the gas velocity dispersion was fixed to the value found in an identical fit to our 2 km s^{-1} cube, using the priors listed in column 2. The prior for the mass-to-light ratio marked with a ⋆ is uniform in logarithmic-space for the free inclination fit, where it covers several orders of magnitude, but it is uniform in linear space for the fixed-inclination fit. This avoids unduly favouring high values.

Некруговые движения газа!

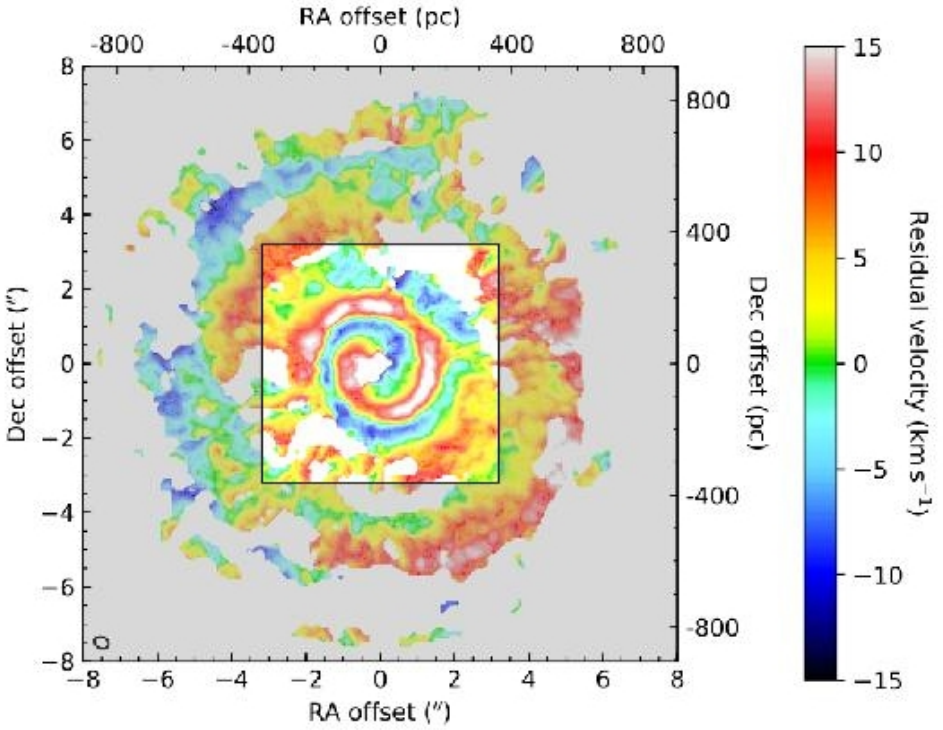

Figure 7. Residuals between the first moments (mean velocity fields) of the data cube and best-fitting model cube. The central box indicates the region within which the model was fit.

Отпустили параметры на волю…

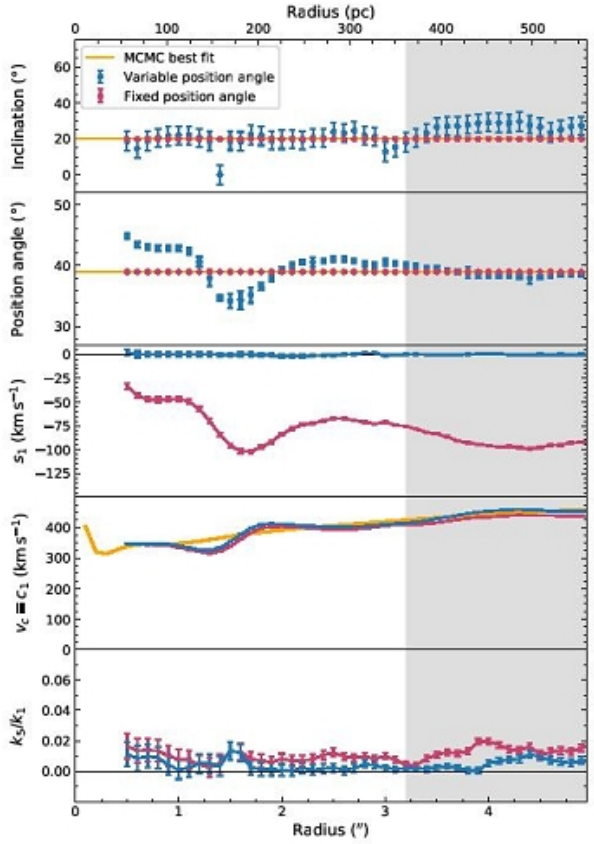

Figure 9. Best-fitting parameters of two harmonic expansions of the observed velocity field, evaluated on ellipses. In blue, the position angles are fit to the velocity field, whereas in red the position angles are fixed to the value used in the full cube fit. The orange line shows the equivalent parameter in the fixed-inclination MCMC fit, while the grey shading shows a radius of 3.″2 that approximates the boundary of the region fit in Section 4.5. **Top panel:** inclinations of the best-fitting ellipses, calculated from Equation 5. **Second panel:** position angles of the best-fitting ellipses. **Third and fourth panels:** first-order coefficients s_1 and c_1, as defined in Equation 4. **Lower panel:** higher-order devia-

- Чисто радиальные движения не проходят.
- Наклон, даже если его отпустить на волю, стоит как вкопанный на 20 градусах.
- Похоже, разворот плоскости газового диска…

ArXiv: 1903.03505

Do Galaxy Morphologies Really Affect the Efficiency of Star Formation during the Phase of Galaxy Transition?

Shuhei Koyama,[1] Yusei Koyama,[2,3] Takuji Yamashita,[1] Masao Hayashi,[4] Hideo Matsuhara,[5,6] Takao Nakagawa,[5] Shigeru V. Namiki,[3] Tomoko L. Suzuki,[4,7] Nao Fukagawa,[3] Tadayuki Kodama,[7] Lihwai Lin,[8] Kana Morokuma-Matsui,[5] Rhythm Shimakawa,[2] and Ichi Tanaka[2]

[1] *Research Center for Space and Cosmic Evolution, Ehime University, 2-5 Bunkyo-cho, Matsuyama, Ehime 790-8577, Japan*

[2] *Subaru Telescope, National Astronomical Observatory of Japan, 650 North A'ohoku Place, Hilo, HI 96720, USA*

[3] *Department of Astronomical Science, Graduate University for Advanced Studies (SOKENDAI), 2-21-1 Osawa, Mitaka, Tokyo 181-8588, Japan*

[4] *National Astronomical Observatory of Japan, 2-21-1 Osawa, Mitaka, Tokyo 181-8588, Japan*

[5] *Institute of Space and Astronautical Science, Japan Aerospace Exploration Agency, 3-1-1 Yoshinodai, Chuo-ku, Sagamihara, Kanagawa 252-5210, Japan*

[6] *Department of Space and Astronautical Science, Graduate University for Advanced Studies (SOKENDAI), 3-1-1 Yoshinodai, Chuo-ku, Sagamihara, Kanagawa 252-5210, Japan*

[7] *Astronomical Institute, Tohoku University, 63 Aramaki, Aoba-ku, Sendai 980-8578, Japan*

[8] *Institute of Astronomy & Astrophysics, Academia Sinica, Taipei 10617, Taiwan*

(Received; Revised; Accepted)

Submitted to ApJ

Выборка из зеленой долины…

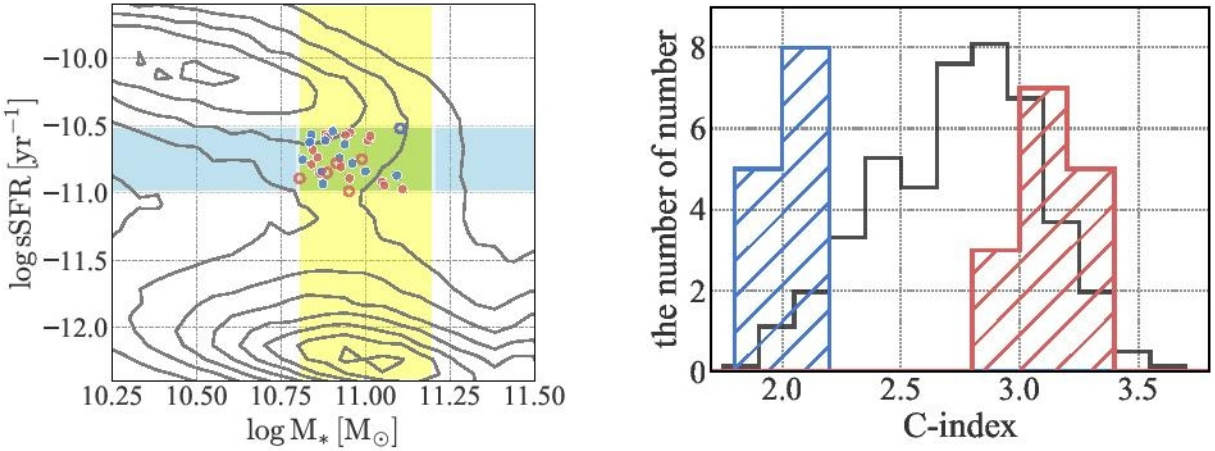

Figure 1. (Left): The stellar mass versus specific SFRs diagram for all SDSS galaxies (gray contours), while the blue and red symbols show the selected disk- and bulge-dominated green-valley galaxies ("disk+green" and "bulge+green", respectively), where the filled and open circles show galaxies from our NRO 45m observations and the xCOLD GASS survey, respectively. The yellow and cyan shaded regions show the M_* and sSFR range applied to select our NRO 45m CO observation target galaxies ($10.8 < \log(M_*/\mathrm{M}_\odot) < 11.2$ and $-11 < \log(sSFR/\mathrm{yr}^{-1}) < -10.5$). (Right): The black histogram shows the arbitrary scaled distribution of C-index for all the SDSS sample with $0.025 < z < 0.05$, $10.8 < \log(M_*/\mathrm{M}_\odot) < 11.2$ and $-11 < sSFR/\mathrm{yr}^{-1} < -10.5$. The blue and red histograms show the distribution of disk-dominated and bulge-dominated green-valley galaxies targeted by our NRO 45m observations, respectively.

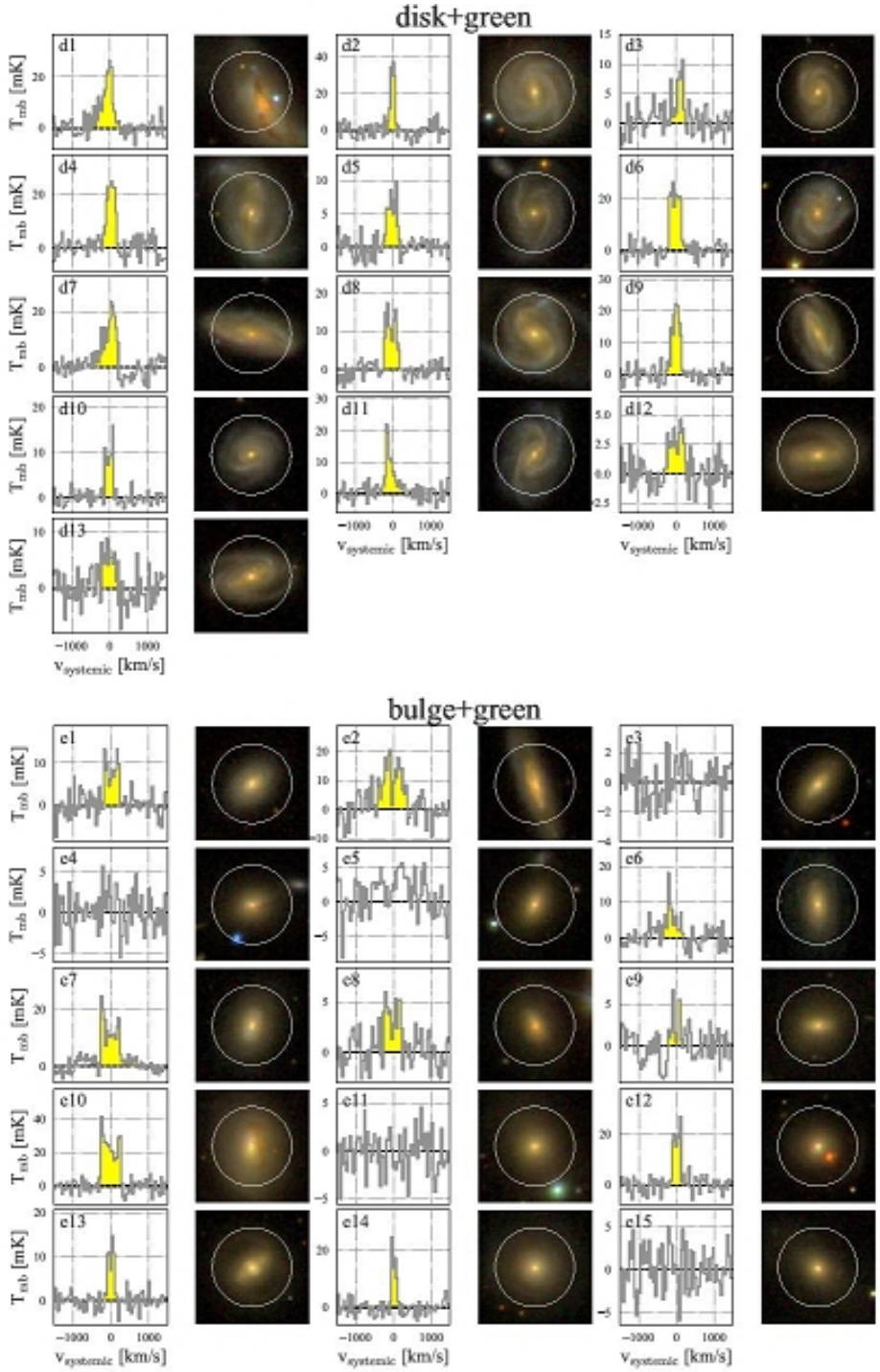
disk+green
d1
d2
d3
d4
d5
d6
d7
d8
d9
d10
d11
d12
d13
bulge+green
c1
c2
c3
c4
c5
c6
c7
c8
c9
c10
c11
c12
c13
c14
c15
T_mb [mK]
v_systemic [km/s]

Распределения параметров для двух подвыборок

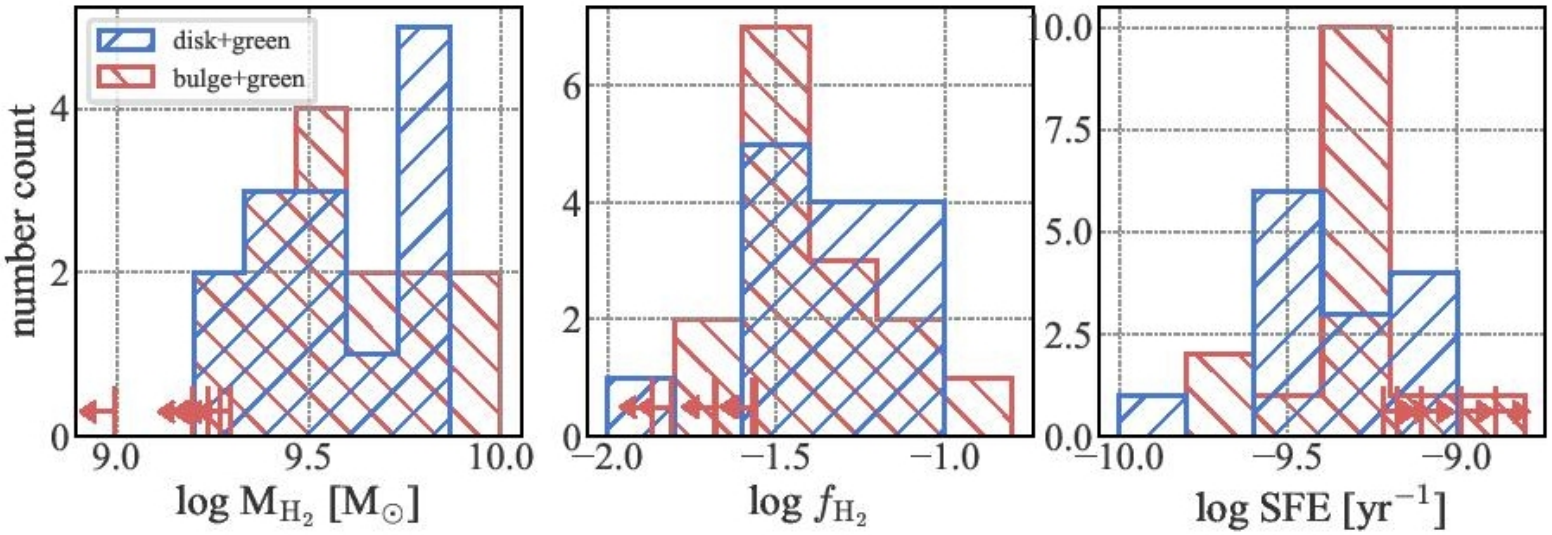

Figure 5. The distributions of M_{H_2} (left), f_{H_2} (middle) and SFE (right) for the disk+green (blue) and bulge+green (red) galaxies. The color coding is the same as that in Figure 4. The red arrows show the upper/lower limits for the CO-undetected bulge+green galaxies, which are not included in the histograms.

Эффективность SF не зависит от присутствия балджа

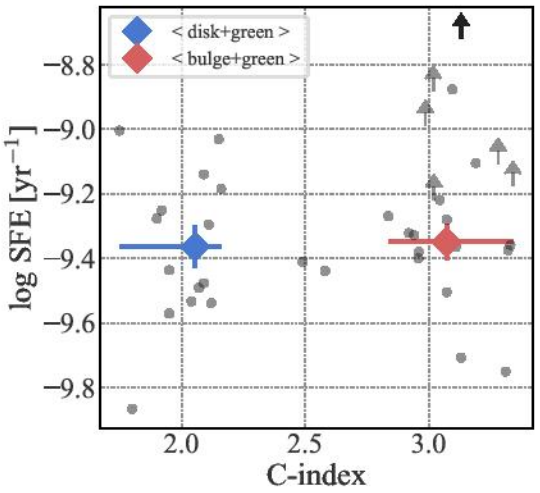

Figure 6. The relation between C-index and SFE at fixed M_* and SFR. For comparison, we also plot two xCOLD GASS sources with intermediate morphology (2.2 < C-index < 2.8) in the same M_*–sSFR window ($10.8 < \log(M_*/\mathrm{M}_\odot) < 11.2$ and $-11 < \log(sSFR/\mathrm{yr}^{-1}) < -10.5$). The gray arrows show the upper limits for the individual CO-undetected sources, while the black arrow indicate the upper limit from their stacking analysis. The blue and red diamonds show the mean SFE for the CO-detected disk+green and bulge+green galaxiess, respectively, where the error bars for the vertical and horizontal axis represent the standard error of the mean

Table 2. Means and standard deviations of $M_{\mathrm{H_2}}$, $f_{\mathrm{H_2}}$ and SFE for the CO-detected disk+green and bulge+green galaxies.

Morphology	log $\mathrm{M_{H_2}}$ [$\mathrm{M}_\odot$]	log $f_{\mathrm{H_2}}$	log SFE [yr^{-1}]
disk-dominated	9.59 ± 0.20	-1.34 ± 0.23	-9.36 ± 0.24
bulge-dominated	9.54 ± 0.25	-1.41 ± 0.25	-9.35 ± 0.22

Если смотреть на голубое облако, то там SFE тоже не зависит от балджа

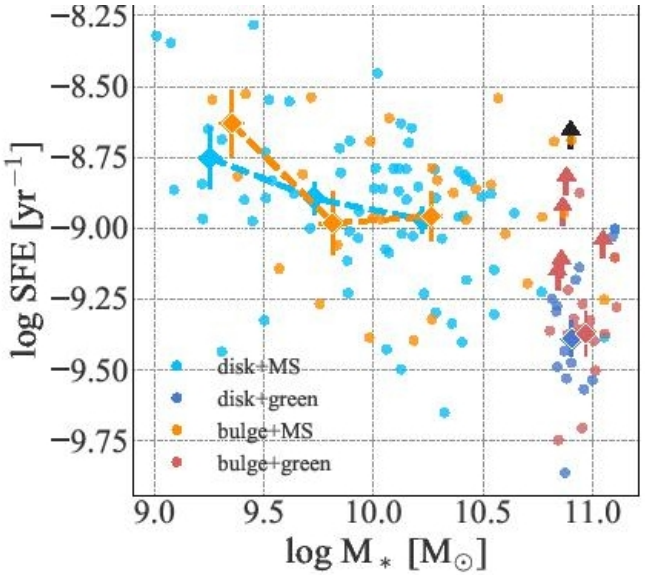

Figure 10. Distribution of galaxies on the M_*–SFE plane for the disk-dominated MS (disk+MS, cyan), disk-dominated green-valley (disk+green, blue), bulge-dominated MS (bulge+MS, orange), and bulge-dominated green-valley galaxies (bulge+green, red). Diamonds and their error bars show the mean and standard deviation for M_* and SFE, where the MS galaxies are divided into three M_* bins ($\log(M_*/M_\odot) = 9.0 - 9.5$, $9.5 - 10.0$ and $10.0 - 10.5$). As for Figure 9-left, the red and black arrows show the lower limits of SFE for CO-undetected bulge+green galaxies and their stacking result, respectively.

K-S соотношение - стандартное

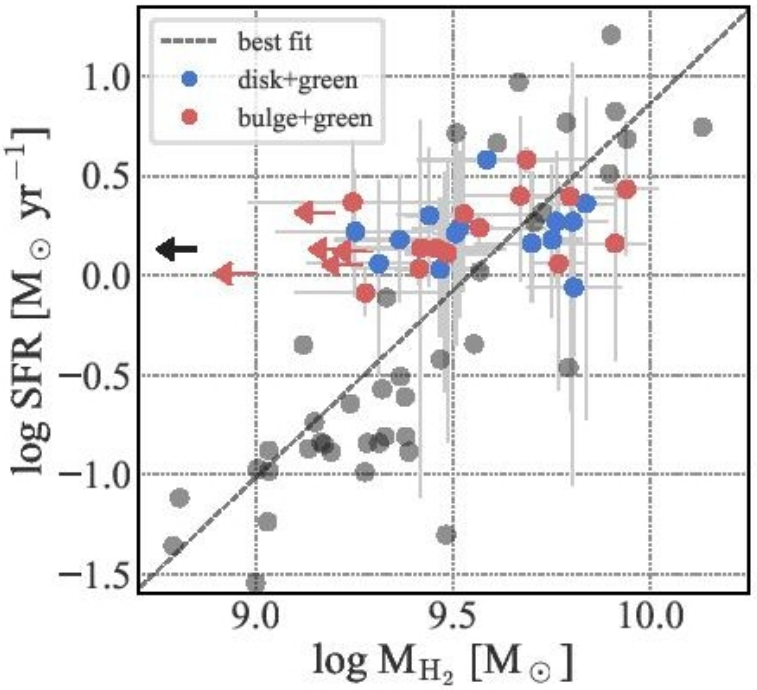

SF по H-alpha

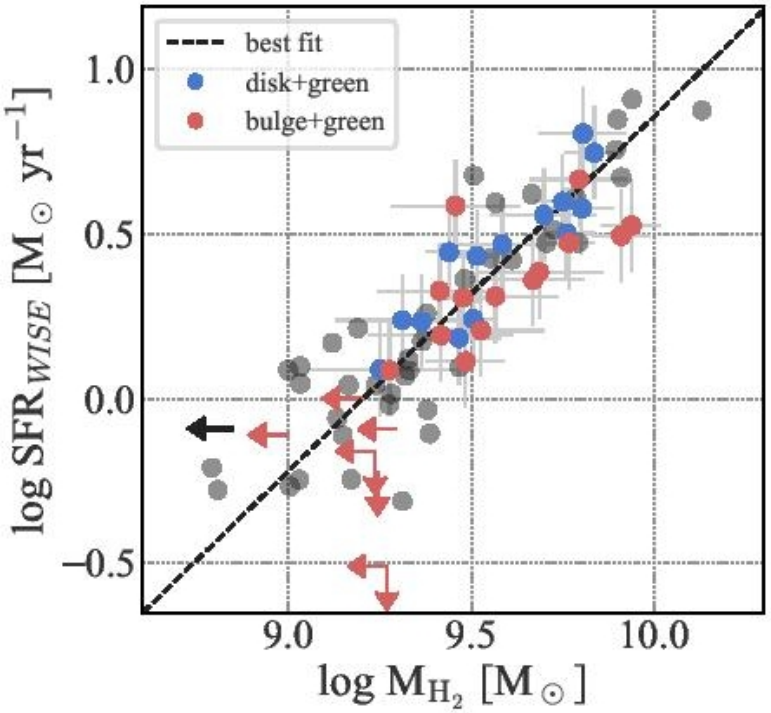

SF по MIR